Chemical Engineering Journal 500 (2024) 156836

Contents lists available at ScienceDirect

Chemical Engineering Journal

journal homepage: www.elsevier.com/locate/cej

Exploring local chlorine generation through seawater electrolysis to Extend optical sensor lifespan in marine environments

T. Matos [a,*], V.C. Pinto [a,b], P.J. Sousa [a,b], M.S. Martins [c], E. Fernández [d], L.M. Goncalves [a,b]

[a] Center for MicroElectromechanical Systems (CMEMS), University of Minho, Campus de Azurém, Guimarães, Portugal
[b] LABBELS –Associate Laboratory, Braga/Guimaraes, Portugal
[c] INESC TEC, Faculdade de Engenharia da Universidade do Porto, Porto, Portugal
[d] Grupo de Oceanografía Biolóxica, Centro de Investigación Mariña, Faculty of Marine Science, Universidade de Vigo, Spain

ARTICLE INFO

Keywords:
Biofouling
Chlorine
Optical sensors
FTO
Platinum nanoparticles, copper
Oceanography

ABSTRACT

Biofouling in marine optical sensors poses a significant challenge as it can compromise data accuracy and instrument functionality. This study investigates the effectiveness of local chlorine generation by seawater electrolysis in mitigating biological fouling and extending the operational lifespan of optical oceanographic instruments. Eight similar turbidity probes integrated with a local chlorine generation system, along with a turbidity probe constructed from ABS and another from PLA with copper filament, were developed for testing in the marine environment. The chlorine probes were designed into two groups: four utilizing standard FTO glass and four featuring FTO glass coated with platinum nanoparticles. Each set of probes employed different excitation currents for chlorine generation. All probes underwent laboratory calibration using formazine before deployment in a coastal environment for 97 days. The findings demonstrate a correlation with higher electrical power leading to prolonged operation intervals free from biofouling interference. Additionally, probes coated with platinum nanoparticles demonstrate higher performance in comparison to those with standard FTO glass. The copper probe did not effectively shield the optical transducers from microfouling, although it effectively demonstrated its efficacy in protecting the structural housing of the device. Overall, this work offers a compelling *in situ* demonstration of local chlorine generation as a promising strategy for enhancing the performance and longevity of optical oceanographic instruments in marine environments.

1. Introduction

Biofouling, the accumulation of microorganisms, algae, plants, or animals on submerged surfaces, poses a significant challenge to environmental sensors. In marine environments, biofouling can swiftly cover sensors, hindering their accuracy and reliability [1]. This accumulation alters the surface properties, interferes with signal transmission, and obstructs sensor functionality [2,3]. The continuous data collection, vital for understanding ocean dynamics and ecosystem functioning, may be compromised by biofouling, leading to erroneous measurements, affecting scientific research and operational activities [4], and potentially leading to flawed conclusions and ineffective management strategies. The importance of addressing biofouling in environmental sensors and oceanography cannot be overstated. Biofouling not only distorts real-time data but also impacts the longevity of sensors and equipment, leading to increased maintenance costs and reduced operational efficiency [5].

Biofouling presents a particularly significant challenge for optical instruments, which rely on the transmission and detection of light to estimate environmental variables such as water clarity, chlorophyll concentration or dissolved organic matter. However, biofouling can rapidly degrade optical sensor performance by coating sensor surfaces with organic matter, thus obstructing light transmission and distorting readings. Mitigating biofouling on optical sensors is imperative to maintain data accuracy and reliability. Strategies such as anti-fouling coatings, mechanical cleaning systems, deployment methods and maintenance protocols can help minimize biofouling effects [6,7]. Additionally, ongoing research into innovative materials and sensor designs aims to develop more robust and biofouling-resistant optical sensors for sustained and high-quality data collection [8–11].

One anti-biofouling technique is based on the use of chlorine. Chlorine, in various forms such as hypochlorite (bleach), chlorine

* Corresponding author.
E-mail address: matos.tiagoandre@cmems.uminho.pt (T. Matos).

https://doi.org/10.1016/j.cej.2024.156836

Available online 19 October 2024

dioxide, or chloramines, is employed to kill or inhibit the growth of microorganisms on sensor surfaces. Chlorine works as an anti-biofouling agent by damaging the cells of biological organisms through its strong oxidizing properties. It disrupts essential cell components, such as proteins and genetic material, which leads to the inhibition of growth and eventual death of the organisms [12,13]. Chlorine can be applied in various ways to prevent biofouling in environmental sensors [14–16]. One common method involves directly injecting chlorine into the water or medium surrounding the sensor. This can be done manually or automatically using dosing pumps controlled by electronic systems. Another approach is coating sensors with materials that slowly release chlorine over time. These coatings ensure a continuous release of chlorine, providing ongoing protection against biofouling. In other cases, sensors may have systems for generating the chemical locally. These systems can use techniques like electrolysis of seawater to produce chlorine on-site. This ensures a steady supply of chlorine for biofouling prevention without relying on external sources.

Some challenges and considerations must be pondered when applying chlorine techniques to environmental sensors. Chlorine can corrode certain materials, so compatibility with sensor components must be ensured. Additionally, it is crucial to balance the concentration of chlorine to effectively prevent biofouling without causing damage to the sensor surface or interfering with sensor measurements. Despite the use of chlorine, biofilms may still form over time, particularly in areas where chlorine concentration may be insufficient or where microbial communities have developed resistance [17–19]. Periodic cleaning and maintenance of sensors may be still required to remove accumulated biofilms, as well as adjustment of chlorine dosage may be necessary to maintain efficacy. While chlorine is effective at preventing biofouling, its long-term environmental impact, particularly in aquatic ecosystems, must be carefully considered. Potential effects on non-target organisms and ecosystem dynamics need to be thoroughly examined and kept under close observation. This includes understanding how chlorine may affect the ecosystem components beyond its immediate anti-biofouling benefits. Control of chlorine dosage is crucial to balance effectiveness with preventing unnecessary environmental damage.

Our research groups aim at developing submersible sensors to continuously monitor the marine environment using cost-effective materials, which, while less resilient to harsh conditions, render them more susceptible to fouling attachment. Notably, most of these devices utilize optical technology, and previous field deployments have demonstrated biofouling interference within a matter of days [20–24]. Consequently, efforts have been directed towards mitigating biological growth on the sensing surfaces.

An initial investigation into effective anti-biofouling methods was undertaken before [25]. In that experiment, six optical turbidity probes were fabricated, and various low-cost and easy-to-apply techniques, based on materials, coatings, and biocides, were examined: (i) structural housing constructed from polylactic acid (PLA); (ii) structural housing constructed from acrylonitrile butadiene styrene (ABS); (iii) structural housing constructed from PLA with copper filament (copper biocide); (iv) in-situ chlorine generation via electrolysis of seawater (chlorine biocide); (v) epoxy coating; and (vi) polydimethylsiloxane (PDMS) coating. These probes were deployed for 41 days in a marine setting to evaluate the impact of biofouling on turbidity measurements. Findings revealed minimal biofouling interference in the chlorine probe throughout the deployment duration, affirming the efficacy of the chlorine generation technique. This new work builds upon the previous investigation and concentrates on the efficiency of chlorine generation. The objective was to assess the minimum chlorine concentration necessary to ensure effective prevention of biofouling *in situ* while reducing power consumption. A lower chlorine release rate into seawater will also mitigate the potential environmental impacts of this anti-fouling technique.

2. Material and methods

The use of chlorine generation stems from the investigation conducted by Pinto et al., which explored the efficacy of employing transparent electrodes composed of fluorine tin oxide (FTO) coated with platinum (Pt) nanoparticles at concentrations of 20 mM (referred to as Pt-FTO) [26]. They empirically evaluated the efficiency of chlorine generation through seawater electrolysis by subjecting 5 cm^2 FTO and Pt-FTO electrode anodes immersed in 50 ml of seawater with approximately 28 g/L of NaCl to three different current injections (200, 300, and 500 μA) over 60 min. Table 1 provides a summary of the hourly chlorine concentration per cm^2 for both FTO and Pt-FTO electrodes as observed in the experimental outcomes. Our research intends to perform a similar experiment with the FTO and Pt-FTO electrodes but applied to environmental instruments and tested in sea-truth scenarios.

2.1. Probes design

The FTO and Pt-FTO electrodes were integrated into optical turbidity probes that use infrared 940 nm transmitted light detection with the optical receiver positioned at a 180° angle from the emitter (principle of turbidimetry [27]). Each probe was 3D printed in acrylonitrile butadiene styrene (ABS) material. The design included two 10 x 30 x 2 mm anode FTO electrodes along with two 4 x 30 x 1 mm cathode electrodes made of stainless steel 316 type (inox) (Fig. 1A). After assembling, the active area of each FTO glass in contact with the water and responsible for the chlorine generation is 15 mm. The chlorine produced is localized on the glass substrate and is quickly dispersed by turbulent flow (which is why a cylindrical sensor housing is used). As a result, chlorine generated at one probe is not expected to interfere with neighbouring probes.

A total of eight turbidity probes were constructed to assess various electrode anodes under different electric currents for chlorine generation: four equipped with FTO electrodes and four with Pt-FTO electrodes. Electric currents of 0, 100, 340, and 540 μA were applied to each set. These current values were selected to align with those employed in the experimental study conducted by Pinto *et al.*, as detailed in Table 1. Despite the similarity in current values, it is essential to acknowledge that variations in electrode design may lead to different chlorine generation outcomes. Pinto *et al.* employed a cathode–anode distance of 2.6 cm, whereas, in our probes, the FTO and inox electrodes are spaced 2 mm apart. Also, the environmental and laboratory conditions are rather different. Two additional probes were incorporated into the setup for comparative purposes: one constructed from ABS without electrodes and another from polylactic acid (PLA) with copper filament (FlashForge PLA Copper 1.75 mm). These control samples were included to assess and contrast with the performance of chlorine techniques. The ABS probe lacks anti-biofouling properties, functioning as a standard sensor without protection, whereas the copper biocide, as demonstrated by previous research [25,28,29], serves as an effective method for preventing biological formation, akin to local chlorine generation. The assembled instrument, featuring the ten turbidity probes (4x FTO-Pt, 4x FTO, 1x ABS and 1x copper), is depicted in Fig. 1B.

Each of the 10 probes utilizes a Vishay Semiconductors VSLY5940 light-emitting diode (LED) and a Vishay Semiconductors BPV11F phototransistor for turbidity measurement. The LED is controlled by an

Table 1
Hourly chlorine concentration per cm^2 for FTO and Pt-FTO electrodes resulted from the experiment of Pinto et al. [26].

Electric current (μA)	Chlorine concentration FTO ($mg.L^{-1}.h^{-1}.cm^{-2}$)	Chlorine concentration Pt-FTO ($mg.L^{-1}.h^{-1}.cm^{-2}$)
200	0.31	1.10
300	0.53	1.60
500	0.70	1.90

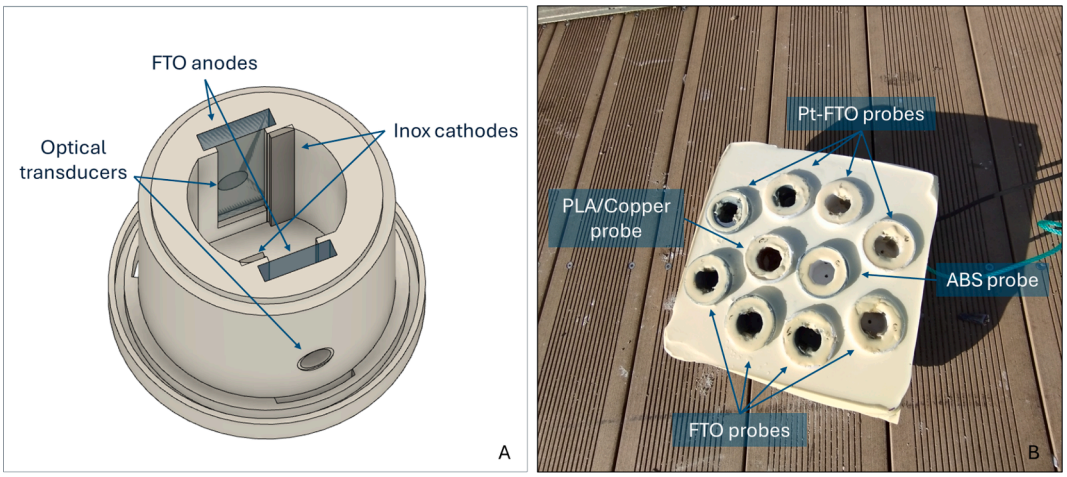

Fig. 1. (A) Scheme of the turbidity probe housing comprising the FTO anodes, inox cathodes and optical transducers. (B) The final instrument used to test the 10 turbidity probes *in situ* (4x FTO, 4x Pt-FTO, 1x ABS and 1x PLA with copper filament).

STM32L051C6T6 microprocessor through a DMG6968U-7 MOSFET for On and Off states. The phototransistor employs a current-to-voltage converter with a gain resistor in series, and the resulting electric signal is read by the microprocessor's analogue-to-digital converter (ADC). The electrodes of each chlorine probe are powered by a 2SC4713KT146R transistor, with their base resistors defining the desired current values (100, 340, and 540 μA). An XC6210B302MR-G regulates the instrument input to 3 V for electronics supply, while an LTC1480 RS485 transceiver is used for RS485 communications. The choice of these electronic components, along with the selection of infrared wavelength to reduce sunlight interference, is based on prior advancements in cost-effective and low-power optical instruments for turbidity and sediment monitoring [20,22–24]. To ensure water resistance, the electronics are encapsulated in polyurethane resin (HB R 16/25—HBQUIMICA). An electric cable, serving both power and RS485 communication, connects the instrument to an external data logger. The complete electronic schematic and printed circuit board (PCB) are provided in Supplementary Material I and II, respectively.

2.2. Turbidity calibration

Before deployment *in situ*, the probes underwent calibration to establish a correlation between their electrical output and turbidity values. A standard formazine solution was employed for this purpose, enabling calibration of the probes into nephelometric turbidity units (NTU). The calibration process involved diluting an initial 4000 NTU solution with distilled water to obtain solutions with lower turbidity. This methodology was presented in previous works with turbidity sensors [20–23]. The probes were immersed in an opaque container with different turbidity solutions. Different dilution factors were used to obtain solutions of 500, 200, 100, 50, 25, 10, 5, and 2.5 NTU. The ratio proportion of the initial and final solutions is given by the following equation:

$$Dilution_{factor} = \frac{volume_{total}}{volume_{initial\_sample}} = \frac{volume_{dilluted\_water} + volume_{initial\_sample}}{volume_{initial\_sample}} \quad (1)$$

Fig. 2 illustrates the calibration outcomes obtained from the turbidity solutions for each probe. The data reveals a notable difference in the shape of the curves between ABS and Copper probes compared to FTO and Pt-FTO probes. This distinction arises from the additional light absorption caused by the FTO glass, while the optical transducers of ABS and Copper probes directly interact with the medium. Other discrepancies in the obtained values across different techniques are attributed to the manual assembly and alignment of the optical transducers. Each calibration curve was embedded in the instrument firmware to convert the electrical output of the probes to a turbidity value during the field experiment. It is worth noting that the presence of biofouling results in a

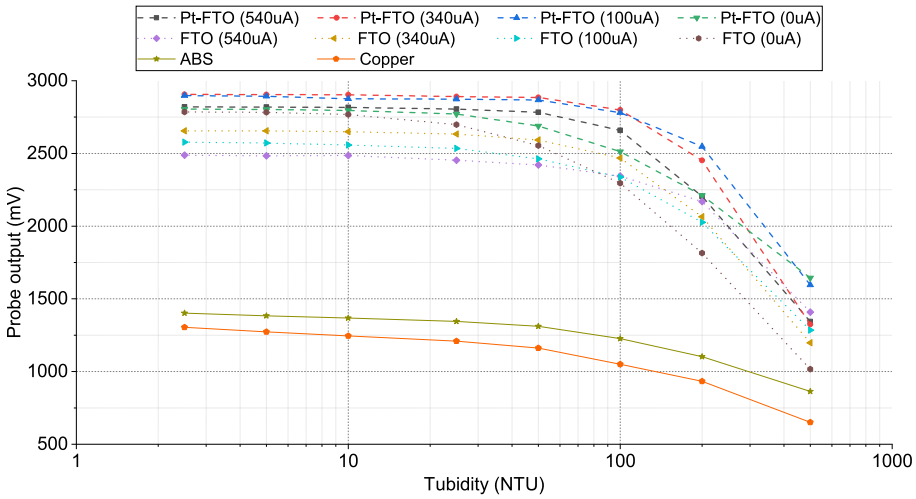

Fig. 2. Calibration results of the ten probes using formazine. The electrical output of each probe is correlated with different turbidity solutions.

reduction of optical power reaching the photodetector, leading to decreased electrical output and elevated turbidity values.

2.3. Field deployment

The instrument was deployed from the 21st of November 2023 to the 25th of February 2024, within the dock of Marine Biological Station at the University of Vigo, situated on Toralla Island in Ria of Vigo, Spain (42°12′07.1″ N 8°47′54.6″ W). The Ria of Vigo is a highly-productive coastal ecosystem, characterized by clear waters and low sedimentary activity, rendering it an ideal site for biofouling assessment [30]. Given these characteristics, fluctuations in water turbidity are anticipated to be negligible. Therefore, an increase in turbidity can be interpreted as biological colonization on the probe surfaces. The prior research on materials, coatings, and chlorine-based anti-biofouling methods was effectively conducted at this location [25].

The instrument was anchored to a floating dock, positioned at a depth of 1.5 m below the water surface, ensuring that the probe apertures faced the seabed to minimize the impact of daylight on measurements. This specific location experiences tidal fluctuations in depth ranging from 3 to 6 m. A connection via an electric cable linked the instrument to a data logger equipped with a real-time clock (RTC) and memory storage, enabling the recording of readings from the ten probes at 30-minute intervals. Power for the entire system was sourced from the electrical grid accessible on the dock. The setup regarding the installation configuration is provided in Supplementary Material III.

2.4. Cleaning methodology

Following two months of experimentation, on the 24th of January 2024, the probes were removed from the water for a cleaning procedure referred to as *in situ* cleaning. This process involved removing macroscopic biofouling adhered to the sensors and gently cleaning the interior of the probes using fresh water and soft cloth. Following *in situ* cleaning, the probes were redeployed to continue the experiment and additional validation of the findings. Upon completion of the experiment, the instrument was transported to the laboratory for hard cleaning. Subsequently, the probes were submerged in a water tank with high chlorine concentration for a period of five days. This process eliminates and dislodges algae from the instrument surfaces. Following the treatment, the interior of the probes underwent a further cleaning with fresh water and soft cloth.

3. Results

The effectiveness of the probes in inhibiting biological formation on the sensor surfaces was assessed using two methods: analysing the turbidity measurements provided by each set of probes throughout the *in situ* experiment and visually examining the probes during and post-test.

3.1. Field measurements

Fig. 3 presents the recorded turbidity of each probe throughout the

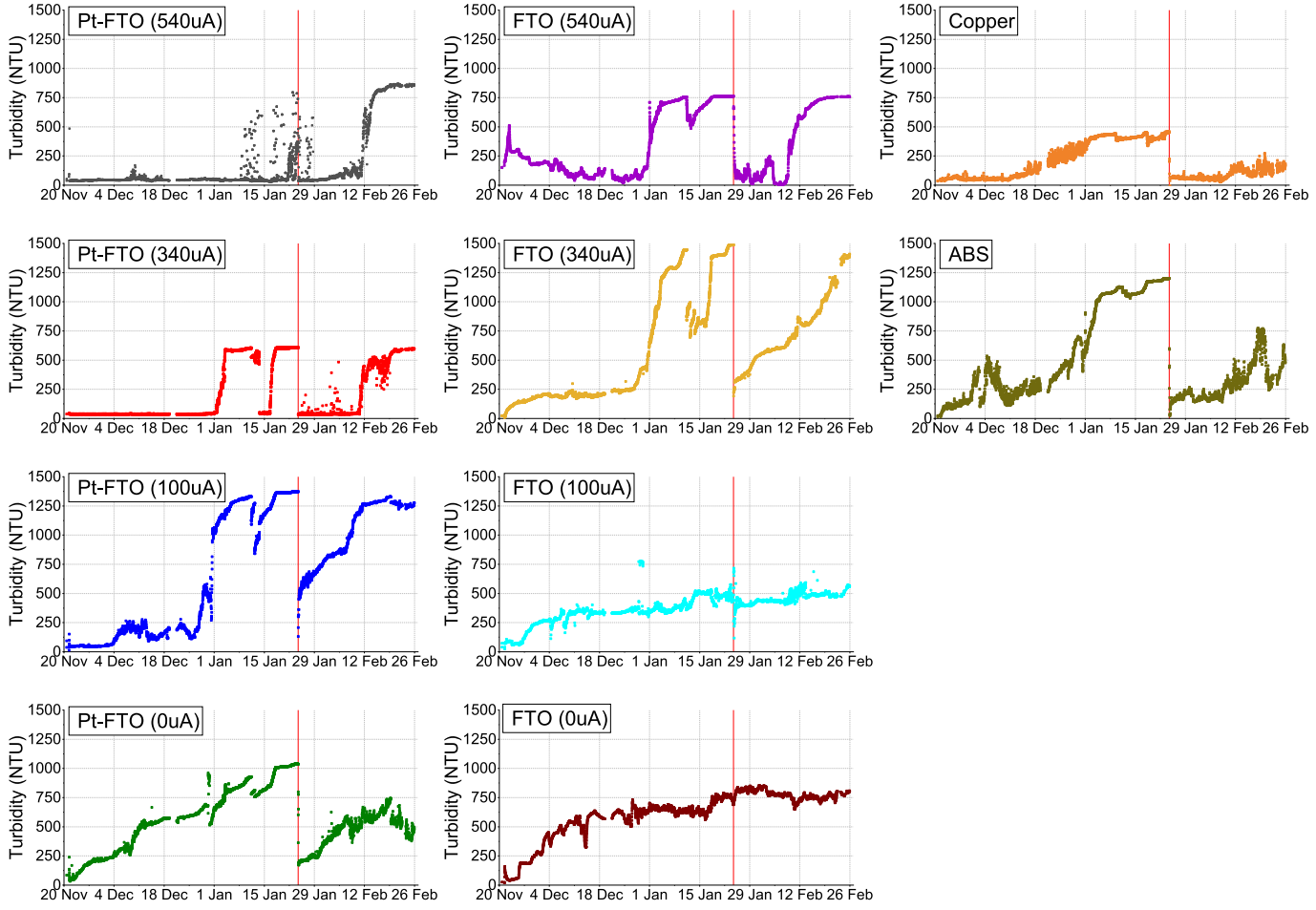

Fig. 3. Turbidity measurements of the ten probes during the *in situ* experiment, from the 21st of November 2023 to the 25th of February 2024, in Ria de Vigo. The vertical red line denotes the date when the probes were removed from the water for *in situ* cleaning (24th of January 2024). (For interpretation of the references to colour in this figure legend, the reader is referred to the web version of this article.)

experiment, spanning from the 21st of November 2023 to the 25th of February 2024. The instrument consistently provided turbidity measurements except for the period between 12 am on the 19th of December and 1 pm on the 21st of December 2023. This interruption was due to a power outage on the dock supplying the monitoring system, which was unrelated to the instrument itself. During this period, the instrument was not removed from the water.

The experiment started on the 21st of November 2023 with all probes measuring turbidity values of 30–60 NTU, except for FTO (540 μA), which measured 130 NTU. Given that the instrument assessed the same water, the turbidity readings of the probes were expected to be similar at the outset of the experiment. Slight variations are expected and attributed to calibration discrepancies. However, the significantly higher turbidity measurement of FTO (540 μA) compared to the other probes suggests an erroneous reading. Possible explanations for this anomaly include dirt on the surface of the FTO glass or the presence of compounds/organisms trapped inside the probe at deployment, that were obstructing the optical channel. Over the subsequent weeks, biological fouling manifested differently across the probes. It is worth reiterating that turbidity in the deployment area was not anticipated to exhibit significant fluctuations in the range of turbidity values observed in our experiment. Therefore, the observed increase in turbidity can be interpreted as interference from biofouling.

The ABS probe, lacking anti-biofouling protection, exhibited a gradual increase in turbidity from the day of deployment onwards. The trend displayed by this probe aligns with expectations for biofouling formation, characterized by continuously rising measurements without reaching steady values, even in the initial days. In contrast, the copper probe, which releases toxic biocides into the water, initially provided consistent and stable turbidity measurements during the first three weeks of deployment. However, beyond this initial period, the measurements began to drift and increase towards higher values.

The four Pt-FTO probes reveal the influence of chlorine generation and its role in preventing biofouling. The Pt-FTO (540 μA) consistently provided reliable turbidity measurements for most of the experiment duration. However, there were two instances of drifting measurements: the first observed on the 21st of January and then on the 11th of February 2024. Additionally, between the 9th and the 29th of January 2024, the probe exhibited sporadic erroneous measurements. This behaviour, which is also observed in probe Pt-FTO (340 μA) from the 26th of January to the 7th of February 2024, is commonly attributed to the presence of macrofouling adhered to the sensor housing. These macrofouling formations, occurring on surfaces unprotected by chlorine, have the potential to encroach upon the sensing area of the probe, causing variable obstructions in the optical channel.

The Pt-FTO (340 μA) probe similarly provided measurements of good quality, comparable to those of Pt-FTO (540 μA). However, between the 2nd to the 24th of January 2024, there were notable spikes in the data, indicating consistent obstruction of the optical channel by macrofouling. It is noteworthy that turbidity sharply increased on the 2nd of January, decreased on the 13th of January, and increased again on the 16th of January 2024. Interestingly, although to varying extents, this pattern was also observed in the data of Pt-FTO (100 μA), Pt-FTO (0 μA), FTO (540 μA), FTO (340 μA), and ABS, all on the same dates. This suggests that the macrofouling across the entire instrument likely impacted these probes uniformly.

The Pt-FTO (100 μA) probe exhibited a slight drift on the 4th of December 2024, which, although minimal, can be indicative of the presence of biofouling. Nonetheless, it still managed to deliver two weeks of uninterrupted, high-quality data. Conversely, the Pt-FTO (0 μA) probe, devoid of chlorine generation, displayed results like those of the ABS probe, with a signal drift noticeable from the day of deployment onward.

Although at a different efficacy level, the FTO probes also underscore the efficacy of chlorine in combating biofouling. The FTO (540 μA) probe initially exhibited a rise in turbidity during the initial days of deployment. Subsequently, the turbidity measurements gradually decreased to levels comparable to the initial turbidity values of 30–60 NTU observed by the other probes at the start of the experiment. This unexpected decrease in turbidity supports the earlier notion proposed to explain the initially measured values of 130 NTU and suggests that the probe might have been fouled to some extent at the time of deployment, and the chlorine produced gradually cleansed the probe over time. On the 30th of December 2023, the probe recorded a sudden spike in turbidity due to biofouling. Remarkably, the FTO (340 μA) experienced a similar surge in turbidity on the same day. However, unlike the FTO (340 μA), which maintained relatively steady values before the 30th of December 2023, its readings were already elevated compared to the initial values measured by the probe. The data at the initial days of deployment of this probe reveals a gradual increase in measured turbidity from the outset, which stabilized after one week of experimentation. Similarly, the turbidity measurements of the FTO (100 μA) also drifted after one week of the experiment. However, the lower chlorine generation of this probe failed to curtail biological growth effectively. The data collected from these probes suggests that the chlorine produced by them was not adequate to entirely prevent the initial formation of biofouling. Still, it did appear to slow down its growth to some extent. In contrast, the FTO (0 μA) did not exhibit signs of anti-biofouling efficacy, demonstrating results akin to other probes lacking protection (ABS and FTO 0 μA), with turbidity increasing since the day of installation.

On the 24th of January, the instrument underwent recovery, during which macrofouling attachments were removed and the interior of the probes was cleaned with fresh water and soft cloth (*in situ* cleaning), before being redeployed into the water. This cleaning process proved effective for Pt-FTO (540 μA), Pt-FTO (340 μA), FTO (540 μA), and copper probes. After cleaning, the measurements from these probes returned to the initial range of 30–60 NTU recorded on the first day of the experiment. The cleaning process also yielded favourable outcomes for Pt-FTO (100 μA), Pt-FTO (0 μA), FTO (340 μA), and ABS probes, resulting in decreased turbidity measurements. However, the values obtained post-cleaning were not identical to those observed at the beginning of the experiment, indicating that microfouling was still present and interfering with the measurements. In contrast, the cleaning was ineffective for FTO (100 μA) and FTO (0 μA) probes, with no alteration in the measurements. Following the cleaning process, the Pt-FTO (540 μA), Pt-FTO (340 μA), and Copper probes delivered two weeks of reliable measurements before exhibiting drift. The FTO (540 μA) probe showed similar results, although with variations during that period. The ABS probe also displayed variations but considering that biofouling interference was already present after cleaning. Pt-FTO (100 μA), Pt-FTO (0 μA), and FTO (340 μA) probes exhibited a gradual increase in turbidity immediately after cleaning.

3.2. Visual inspections

Visual inspections were carried out to qualitatively compare the level of biofouling on the probes at various stages of the experiment, with a specific focus on macro-biofouling assessment. Photographs of each probe were captured before deployment, on the 21st of December 2023, before and after *in situ* cleaning on the 24th of January 2024, and on the recovery day on the 25th of February 2024. The top image in Fig. 4 presents the condition of each probe at the different time points during the field experiment.

The first visual inspection took place one month after the beginning of the experiment, on the 21st of December 2023 (second row of the top image in Fig. 4). At this point, the probes displayed signs of macrofouling on their surfaces. However, the sensing areas of the probes appeared clean to the naked eye. The instruments were redeployed in their current state without undergoing any cleaning procedure. On the 24th of January 2024, the probes were removed from the water for the second inspection. The third row of photographs depicted in the top

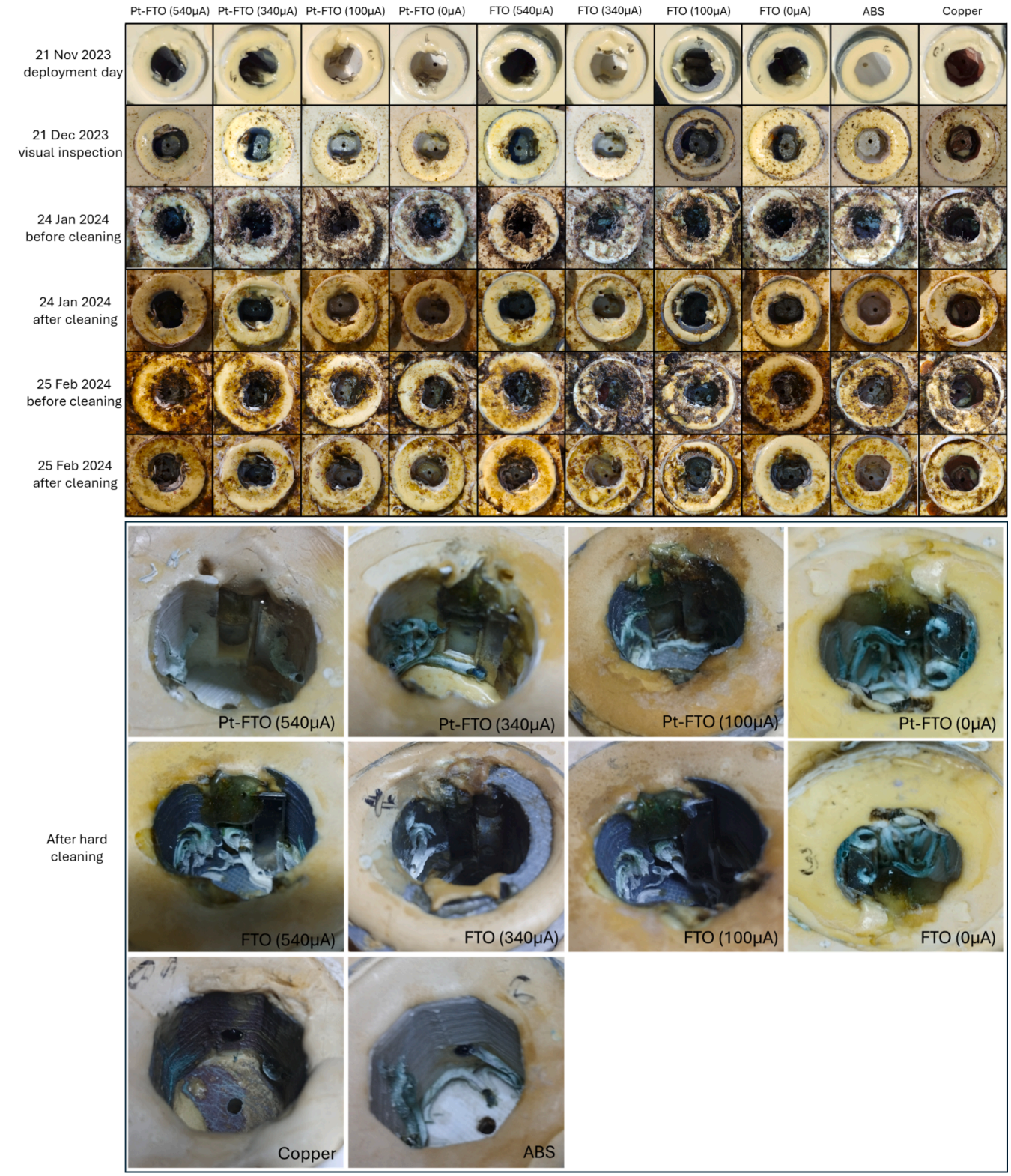

Fig. 4. On the top, photographs of the probes at different stages of the experiment: before deployment (21 Nov 2023), after one month of the experiment (21 Dec 2023), after and before the *in situ* cleaning on 24 Jan 2024 and on the recovery day after and before the *in situ* cleaning (25 Feb 2024). On the bottom are displayed photographs of the probes after hard cleaning.

image of Fig. 4 reveals increasing biological growth on the substrates, resulting in interference within the sensing areas. At this stage, biofouling was evident in the instruments, including the interiors of each probe. The macro fouling was removed and the sensing areas were cleaned using fresh water and a soft cloth (*in situ* cleaning, fourth row of photographs in the top image of Fig. 4). Upon recovery, on the 25th of February 2024, the instrument exhibited persistent signs of biofouling throughout its entirety (fifth row of photographs in the top image of Fig. 4). The *in situ* cleaning procedure was handled to eliminate the macro-fouling adhered to the instrument (sixth row of photographs in

the top image of Fig. 4).

Following the experiment, the instrument underwent a rigorous cleaning process in the laboratory. It was submerged in a tank with high chlorine concentration for five days (hard cleaning) to dislodge macrofouling and eradicate existing micro-fouling organisms. Subsequently, the device was cleaned using fresh water and soft cloth in preparation for the final visual inspection (depicted in the bottom image of Fig. 4). Following the hard cleaning, biofouling was eliminated except for limestone tubes built by polychaetes organisms. These limestone formations were attached all over the instrument, including the interior of the probes, except for the copper probe (bottom image of Fig. 4). Pt-FTO (540μA) and Pt-FTO (340μA) chlorine probes were notable for exhibiting clean glass substrates on both transducers. Despite limestone tube growth inside both probes, it was observed only around the glasses that remained clean due to the localized chlorine generation. Pt-FTO (100μA) and FTO (540μA) exhibited one clean glass and the other one obstructed by limestone structures. All the other chlorine probes presented both glass substrates partially or totally blocked by the limestone structures. The chlorine generation was not sufficient to prevent the limestone formations on these probes. Additionally, the ABS probe, lacking anti-biofouling properties, also experienced limestone formation partially covering the optical.

4. Discussion

The conducted field experiment using the developed probes aimed to evaluate the excitation current required for chlorine generation to counteract biological growth on the instrument's sensing areas. While higher electric currents yield elevated chlorine concentration, factors such as power consumption, battery constraints, and ecological considerations limit their practical application. This study confirmed the effectiveness of using chlorine to prevent biofouling and demonstrated a direct relationship between the electric power used for its generation and the prolonged operation time without cleaning needs.

Fig. 5 illustrates the operational time without biofouling interference for FTO-Pt and copper probes during the field experiment. The number of reliable days was counted from the deployment day until consecutive measurements indicated a 20 % increase from the initial values. The probe with the highest chlorine generation, Pt-FTO (540 μA), exhibited minimal biofouling effects and provided reliable measurements without requiring cleaning for 65 days. Following closely, the Pt-FTO (340 μA) probe yielded 41 days of high-quality data. Concerns were raised regarding the actual effectiveness of this probe, as biofouling interference observed after the 1st of January seemed to be linked to macrofouling outside the sensing area, suggesting the potential for extended operation time. Subsequently, the copper probe demonstrated 20 days of reliable performance, followed by the Pt-FTO (100 μA) probe with 11 days, both considered acceptable results within a marine environment. Conversely, the remaining probes did not meet the expected criteria for effective biofouling prevention. Although the FTO (540 μA) probe was anticipated to exhibit some efficacy, unexpected turbidity spikes during the initial days of the experiment hindered its overall assessment. The experiment validated that FTO glass performs better with platinum coating. Previous laboratory studies by Vania *et al.* demonstrated that chlorine generation is higher for Pt-FTO under the same excitation current [26]. Our results further support this assertion, as the Pt-FTO probes (540 μA, 340 μA, and 100 μA) outperformed the FTO probes (540 μA, 340 μA, and 100 μA).

A previous work testing chlorine generation, along with other anti-biofouling techniques, including copper, was conducted in the Ria of Vigo from the 23rd of May to the 9th of July 2022 [25]. In this test, a chlorine probe (excitation current of 350 μA) similar to those utilized in the current experiment surpassed its competitors, providing 41 days of consistent measurements. The Pt-FTO (540 μA) probe exceeded this duration by an additional 24 days. However, it is important to note that this new experiment took place during a period of minimal marine primary production within the seasonal cycle, characterized by relatively low colonization of hard substrates by new recruits delivered by benthic organisms naturally inhabiting the Ría de Vigo. By contrast, the previous experiment in 2022 occurred at the start of summer when marine production and biofilm formation are expected to be higher. For comparison, identical copper probes were employed in both experiments. In the 2022 experiment, the copper probe remained free of biofouling interference for 15 days, compared to 20 days achieved in this new deployment.

The visual inspections revealed a correlation with the data presented during the deployment phase. Following hard cleaning, only the Pt-FTO (540 μA) and Pt-FTO (340 μA) probes exhibited clear FTO glass surfaces devoid of limestone tubes. The chlorine generation was insufficient to shield the sensor housing, but the sensing areas remained protected. In contrast, the copper probe was completely clean, with no traces of limestone tubes, and consistently exhibited fewer macrofouling traces during all visual inspections throughout the deployment. This behaviour was also observed during the 2022 tests. The biocidal properties of copper proved to be effective in protecting the structural housing but were insufficient to safeguard the transducers' surfaces from micro-fouling since they are in permanent contact with water.

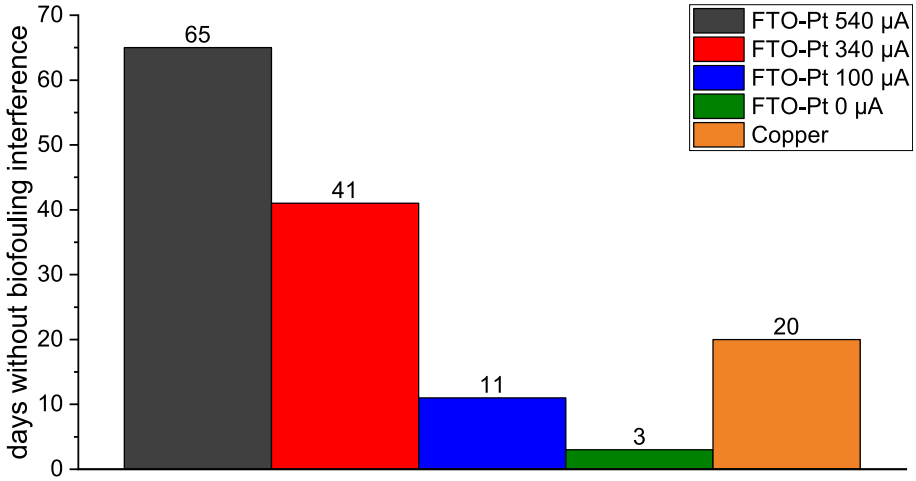

Fig. 5. Days of reliable measurement without biofouling interference during the field experiment. Days were counted from the deployment day until consecutive measurements showed a 20% increase from the initial values. FTO probes were excluded due to insufficient chlorine generation to prevent biofouling interference.

5. Conclusion

This work presents the development and implementation of optical turbidity sensors equipped with an anti-biofouling technique involving local chlorine generation. The instruments utilize transparent FTO glass substrates to shield the optical transducers and generate chlorine through the electrolysis of seawater. Eight probes were constructed with the following setup: four probes with standard FTO glass and excitation currents of 540, 340, 100, and 0 μA, and four probes with FTO glass coated with platinum nanoparticles (Pt-FTO) using the same excitation currents. Additionally, two probes constructed from ABS and PLA with copper filament were included for comparative analysis. Laboratory calibration using formazine solution was conducted to establish the correlation between their electrical output and turbidity measurements in NTU. Subsequently, the probes were deployed in a coastal environment characterized by low sedimentary activity and high primary production from the 21st of November 2023 to the 25th of February 2024. Different cleaning procedures were employed during and after the experiment, and visual inspections were documented to assess macrofouling and compare devices' performance.

The obtained results demonstrate a clear correlation between the excitation current and the efficacy in preventing biological fouling. Utilizing higher electrical power for chlorine generation led to extended measurement periods free from biofouling interference. A lifespan of 65 days for FTO-Pt with a 500 μA excitation current without biofouling interference and need for cleaning was estimated. Additionally, the application of platinum nanoparticle coating, which substantially enhances chlorine generation, resulted in higher performance of the Pt-FTO probes compared to the FTO probes. Moreover, the copper probe exhibited effectiveness as an anti-biofouling technique, achieving 20 days of operation without biofouling interference. Although safeguarding optical areas is not feasible due to its lack of transparency, protecting the sensor housing proved to be a valuable resource for other sensor types and applications. The use of copper housing proved effective in preventing macrofouling, suggesting that combining chlorine generation with copper housing can protect both the optical areas and the structural components, thereby improving results.

This study serves as a compelling demonstration of the efficacy of local chlorine generation in prolonging the operational lifespan of optical oceanographic instruments by delaying biological fouling. The use of higher electrical power for water electrolysis correlates with extended operation intervals without requiring cleaning. Determining the optimal excitation current for chlorine generation must consider the intended application, finding a balance between required operation time and available energy supply (often batteries), while also mitigating environmental impact. Our experiment analysed the operation time of every probe without biofouling interference. While the achieved durations can serve as illustrative examples, they should not be viewed as strict references. Variations in probe designs, seasonal conditions, deployment configurations, and marine environmental factors are likely to yield diverse outcomes. Moreover, chlorine-resistant microorganisms can pose additional challenges to the long-term effectiveness of the presented technique. Biofouling remains the primary challenge affecting the operational longevity of environmental sensors used for continuous monitoring in aquatic environments. Enhancing biofouling prevention techniques is essential to improve the reliability of these instruments, paving the way for the next generation of *in situ* oceanographic sensors.

CRediT authorship contribution statement

T. Matos: Writing – review & editing, Writing – original draft, Validation, Methodology, Investigation, Formal analysis, Data curation, Conceptualization. **V.C. Pinto:** Writing – review & editing, Methodology. **P.J. Sousa:** Writing – review & editing, Methodology. **M.S. Martins:** Writing – review & editing, Supervision, Project administration. **E. Fernández:** Writing – review & editing, Validation, Resources. **L.M. Goncalves:** Writing – review & editing, Validation, Supervision, Project administration.

Funding

This work is co-funded by national funds through FCT–Fundação para a Ciência e a Tecnologia, I.P., under project SONDA (PTDC/EME-SIS/1960/2020) and PlastiSensor (PTDC/EAM-OCE/6797/2020).

Declaration of competing interest

The authors declare that they have no known competing financial interests or personal relationships that could have appeared to influence the work reported in this paper.

Acknowledgements

The authors thank Estación de Ciencias Mariñas de Toralla (ECIMAT) for the support during the field experiments. T.M thanks IACOBUS Estadias de Investigação 2024, managed by AECT Galicia-Norte de Portugal, co-financed with FEDER funds through the INTERREG Spain-Portugal (POCTEP) 2021-2027. Vânia Pinto and Paulo Sousa thank FCT for their contracts funding provided through 2021.01087.CEECIND (https://doi.org/10.54499/2021.01087.CEECIND/CP1664/CT0020) and 2021.01086.CEECIND (https://doi.org/10.54499/2021.01086.CEECIND/CP1664/CT0008), respectively.

Appendix A. Supplementary data

Supplementary data to this article can be found online at https://doi.org/10.1016/j.cej.2024.156836.

Data availability

No data was used for the research described in the article.

References

[1] G. D. Bixler and B. Bhushan, "Biofouling: lessons from nature," *Philos. Trans. R. Soc. A Math. Phys. Eng. Sci.*, vol. 370, no. 1967, pp. 2381–2417, May 2012, doi: 10.1098/RSTA.2011.0502.
[2] Y.T. Chen, J. Crossman, The impacts of biofouling on automated phosphorus analysers during long-term deployment, Sci. Total Environ. 784 (2021) 147188, https://doi.org/10.1016/J.SCITOTENV.2021.147188.
[3] S. Bhatia, et al., Biofouling of an all-optical sensor for seafloor monitoring of marine carbon capture and storage sites, Energy Procedia 63 (2014) 3848–3852, https://doi.org/10.1016/J.EGYPRO.2014.11.414.
[4] A. Kerr, et al., The early stages of marine biofouling and its effect on two types of optical sensors, Environ. Int. 24 (3) (1998) 331–343, https://doi.org/10.1016/S0160-4120(98)00011-7.
[5] R. Venkatesan, P. Senthilkumar, N. Vedachalam, P. Murugesh, Biofouling and its effects in sensor mounted moored observatory system in Northern Indian Ocean, Int. Biodeterior. Biodegradation 116 (2017) 198–204, https://doi.org/10.1016/J.IBIOD.2016.10.034.
[6] A. Whelan, F. Regan, Antifouling strategies for marine and riverine sensors, J. Environ. Monit. 8 (9) (2006) 880–886, https://doi.org/10.1039/B603289C.
[7] L. Delauney, C. Compare, M. Lehaitre, Biofouling protection for marine environmental sensors, Ocean Sci. 6 (2) (2010) 503–511, https://doi.org/10.5194/OS-6-503-2010.
[8] C. Sanchez-Cano and M. Carril, "Recent Developments in the Design of Non-Biofouling Coatings for Nanoparticles and Surfaces," *Int. J. Mol. Sci. 2020, Vol. 21, Page 1007*, vol. 21, no. 3, p. 1007, Feb. 2020, doi: 10.3390/IJMS21031007.
[9] L. Zhang, H. Li, X. Zhang, Q. Li, G. Zhu, F.Q. Liu, A marine coating: Self-healing, stable release of Cu2+, anti-biofouling, Mar. Pollut. Bull. 195 (2023) 115524, https://doi.org/10.1016/J.MARPOLBUL.2023.115524.
[10] S. Kumar, F. Ye, S. Dobretsov, J. Dutta, Nanocoating is a new way for biofouling prevention, Front. Nanotechnol. 3 (2021) 771098, https://doi.org/10.3389/FNANO.2021.771098/BIBTEX.
[11] A. Ali, E.T. Kang, L. Xu, Nature-inspired anti-fouling strategies for combating marine biofouling, Prog. Org. Coatings 189 (2024) 108349, https://doi.org/10.1016/J.PORGCOAT.2024.108349.
[12] W. Gottardi, M. Nagl, Chlorine covers on living bacteria: the initial step in antimicrobial action of active chlorine compounds, J. Antimicrob. Chemother. 55 (4) (2005) 475–482, https://doi.org/10.1093/JAC/DKI054.

[13] D. Ghernaout, A. Alghamdi, B. Ghernaout, Microorganisms' killing: chemical disinfection vs. electrodisinfection, Electrodisinfection. Appl. Eng. 3 (1) (2019) 13–19, https://doi.org/10.11648/J.AE.20190301.12.
[14] L. Delauney and C. Compère, "An Example: Biofouling Protection for Marine Environmental Sensors by Local Chlorination," *Springer Ser. Biofilms*, pp. 1–16, 2008, doi: 10.1007/7142_2008_9.
[15] D. Laurent *et al.*, "Biofouling protection by electro-chlorination on optical windows for oceanographic sensors and imaging devices," *MTS/IEEE Ocean. 2015 - Genova Discov. Sustain. Ocean Energy a New World*, Sep. 2015, doi: 10.1109/OCEANS-GENOVA.2015.7271715.
[16] S. Lou, P. Wang, B. Ma, J. Wu, D. Zhang, Biofouling protection for marine optical windows by electrolysis of seawater to generate chlorine using a novel Co-based catalyst electrode, Colloids Surfaces A Physicochem. Eng. Asp. 638 (2022) 128270, https://doi.org/10.1016/J.COLSURFA.2022.128270.
[17] I.Y. Roi, N.A. Klimenko, G.M. Zdorovenko, V.V. Goncharuk, Species identification of water microorganisms resistant to chlorine compounds, J. Water Chem. Technol. 37 (3) (2015) 145–150, https://doi.org/10.3103/S1063455X1503008X/METRICS.
[18] L.W. Luo, et al., Evaluating method and potential risks of chlorine-resistant bacteria (CRB): A review, Water Res. 188 (2021) 116474, https://doi.org/10.1016/J.WATRES.2020.116474.
[19] M. Rajeev, T.J. Sushmitha, K.G. Prasath, S.R. Toleti, S.K. Pandian, Systematic assessment of chlorine tolerance mechanism in a potent biofilm-forming marine bacterium Halomonas boliviensis, Int. Biodeterior. Biodegradation 151 (2020) 104967, https://doi.org/10.1016/J.IBIOD.2020.104967.
[20] T. Matos, C. L. Faria, M. Martins, R. Henriques, and L. Goncalves, "Optical device for in situ monitoring of suspended particulate matter and organic/inorganic distinguish," in *OCEANS 2019 - Marseille, OCEANS Marseille 2019*, Jun. 2019, vol. 2019-June, doi: 10.1109/OCEANSE.2019.8867080.
[21] T. Matos, et al., A low-cost, low-power and low-size multi-parameter station for real-time and online monitoring of the coastal area, Ocean. Conf. Rec. 2022 (2022), https://doi.org/10.1109/OCEANS47191.2022.9977347.
[22] T. Matos, C.L. Faria, M.S. Martins, R. Henriques, P.A. Gomes, L.M. Goncalves, Development of a cost-effective optical sensor for continuous monitoring of turbidity and suspended particulate matter in marine environment, Sensors 19 (20) (2019) 4439, https://doi.org/10.3390/s19204439.
[23] T. Matos, C.L. Faria, M.S. Martins, R. Henriques, P.A. Gomes, L.M. Goncalves, Design of a multipoint cost-effective optical instrument for continuous in-situ monitoring of turbidity and sediment, Sensors 20 (11) (2020) 3194, https://doi.org/10.3390/s20113194.
[24] T. Matos, J.L. Rocha, C.L. Faria, M.S. Martins, R. Henriques, L.M. Goncalves, Development of an automated sensor for in-situ continuous monitoring of streambed sediment height of a waterway, Sci. Total Environ. 808 (2022) 152164, https://doi.org/10.1016/J.SCITOTENV.2021.152164.
[25] T. Matos *et al.*, "Design and In Situ Validation of Low-Cost and Easy to Apply Anti-Biofouling Techniques for Oceanographic Continuous Monitoring with Optical Instruments," *Sensors 2023, Vol. 23, Page 605*, vol. 23, no. 2, p. 605, Jan. 2023, doi: 10.3390/S23020605.
[26] V.C. Pinto, P.J. Sousa, E.M.F. Vieira, L.M. Gonçalves, G. Minas, Antibiofouling strategy for optical sensors by chlorine generation using low-cost, transparent and highly efficient electrodes based on platinum nanoparticles coated oxide, Chem. Eng. J. 404 (2021) 126479, https://doi.org/10.1016/J.CEJ.2020.126479.
[27] T. Matos, M.S. Martins, R. Henriques, L.M. Goncalves, A review of methods and instruments to monitor turbidity and suspended sediment concentration, J. Water Process Eng. 64 (Jul. 2024) 105624, https://doi.org/10.1016/J.JWPE.2024.105624.
[28] S.J. Brooks, M. Waldock, Copper Biocides in the Marine Environment, Ecotoxicol. Antifouling Biocides (2009) 413–428, https://doi.org/10.1007/978-4-431-85709-9_24.
[29] S. Brooks and M. Waldock, "The use of copper as a biocide in marine antifouling paints," *Adv. Mar. Antifouling Coatings Technol.*, pp. 492–521, Jan. 2009, doi: 10.1533/9781845696313.3.492.
[30] E. Fernández, X.A. Álvarez-Salgado, R. Beiras, A. Ovejero, G. Méndez, Coexistence of urban uses and shellfish production in an upwelling-driven, highly productive marine environment: The case of the Ría de Vigo (Galicia, Spain), Reg. Stud. Mar. Sci. 8 (2016) 362–370, https://doi.org/10.1016/J.RSMA.2016.04.002.